Assessment of RANS Turbulence Models in Urban Environments: CFD Simulation of Airflow Around Idealized High-Rise Morphologies

Farshid Kardan[1,2(✉)], Olivier Baverel[2], and Fernando Porté Agel[1]

[1] Wind Engineering and Renewable Energy Laboratory (WIRE), Ecole Polytechnique Fédérale de Lausanne (EPFL), Lausanne, Switzerland
farshid.kardan@epfl.ch
[2] Laboratoire GSA-Géométrie Structure Architecture (Ecole Nationale Supérieure D'architecture Paris-Malaquais), University Paris-Est, Paris, France

Abstract. This paper presents the evaluation of Reynolds-averaged NavierStokes (RANS) turbulence models, including the RNG $k - \varepsilon$, SST $k - \omega$ and more recently developed SST $\gamma - Re_\theta$ models of flow past an idealized three-dimensional urban canopy. For validation purposes, the simulated vertical and spanwise profiles of mean velocity are compared with wind tunnel measurements and large eddy simulation (LES) results. These quantitative validations are essential to assess the accuracy of RANS turbulence models for the simulation of flow in built environments. Furthermore, additional CFD simulations are performed to determine the influence of three different idealized high-rise morphologies on the flow within and above the semi-idealized urban canopy. In order to assess airflow behavior, the pressure coefficient on high-rise morphologies, turbulence kinetic energy contours and vertical velocity magnitude profiles at roof level of high-rise and surrounding buildings are evaluated. The results render the SST $\gamma - Re_\theta$ model attractive and useful for the simulation of flows in real and complex urban morphologies. For the region around an idealized high-rise building, different flow patterns and strong changes in velocity magnitude and pressure coefficient are observed for different building morphologies.

Keywords: Computational fluid dynamics (CFD) · RANS models · Idealized urban canopy · Building morphologies

1 Introduction

The fast and accurate prediction of turbulent airflow in built environments is becoming increasingly essential to architectural and urban projects. Three main approaches can be used to study airflow in urban environments: full-scale measurements, reduced-scale wind tunnel experiments and computational fluid dynamics (CFD). (i) Full-scale measurement is the most accurate method, as it utilizes the physical and real scale objects. However, it is expensive and time-consuming, which makes it impractical in many situations. (ii) Reduced-scale wind tunnel experimentation is comparatively

K. De Rycke et al., *Humanizing Digital Reality*,
https://doi.org/10.1007/978-981-10-6611-5_23

faster and less expensive than the full-scale measurement method, but the analyzing process is generally limited to a few selected discrete positions in the flow field, which can make it difficult to study a large and complex environment like an urban canopy. (iii) Computational fluid dynamics (CFD) provide a time and cost effective method to study and predict turbulent flows. CFD is particularly useful to forecast urban meteorological phenomena, estimate the dispersion of air pollutants, predict fire spreading, evaluate the urban heat island effect, optimize the outdoor and indoor thermal environments, maximize the wind comfort and safety around buildings, calculate the wind loads on building structures, improve the indoor air quality by natural ventilation, and optimize the harvesting of solar and wind energy in built environments (Moonen et al. 2012; Nakayama et al. 2011; Stankovic et al. 2009).

In general, there are three main types of CFD methods (Ferziger and Peric 1997; Pope 2000): (i) direct numerical simulation (DNS), (ii) large-eddy simulation (LES) and (iii) Reynolds-averaged Navier-Stokes (RANS). The RANS simulations are highly sensitive to the choice of turbulence model, but have the advantage of having a substantially lower computational cost compared to DNS and LES. For this reason, RANS remains the CFD tool of choice for many applications, particularly those involving short-time forecasts and large-scale simulations, which can be highly computationally demanding. Considering the variety of RANS turbulence models available in the literature and the sensitivity of the results to the choice of turbulence model, a rigorous evaluation of said models is needed (Liu et al. 2013; Liu and Niu 2016; Tominaga and Stathopoulos 2013). For this purpose, a comprehensive comparison of three RANS turbulence models is conducted including the re-normalisation group (RNG) $k - \varepsilon$ (Yakhot et al. 1992), shear-stress transport (SST) $k - \omega$ (Menter 1994) and SST $\gamma - Re_\theta$ (Langtry and Menter 2009) models for flow over an idealized three-dimensional urban canopy by comparing the simulation results with the wind tunnel measurements of Brown et al. (2001) and the large-eddy simulation results of Cheng and Porté-Agel (2015). Recently, Kardan et al. (2016) conducted a detailed evaluation of RANS turbulence models for flow over a two-dimensional isolated building, and reported a relatively better performance of the SST $k - \omega$ and SST $\gamma - Re_\theta$ models in both unstructured and coarse grid resolution. However, it is also reported that further investigation into complex three-dimensional urban environments is needed to generalize the SST models' results.

High-rise buildings have become increasingly prevalent in cities as an inevitable result of population growth and lack of available land in urban areas. Since rectangular prisms, cylinders, and twisting forms are some of the most common geometries found in high-rise building designs, it is essential to assess how building morphologies affect wind behavior around such structures. In this study, following the evaluation and selection of an appropriate RANS turbulence model, additional CFD simulations are conducted to determine the effect of the aforementioned high-rise morphologies on the flow above the semi-idealized urban canopy. In order to assess the wind behavior on and around buildings, the pressure coefficient distribution, turbulent kinetic energy (TKE) and vertical profiles of velocity magnitude at roof level of high-rise and sur-rounding buildings are evaluated.

2 Numerical Setup

The simulations were performed on the Deneb cluster using the high-performance computing (HPC) unit of Swiss Federal Institute of Technology in Lausanne (EPFL). A total of 64 CPUs (Intel Xeon) were used in parallel for the simulations.

Idealized Urban Canopy Case

The CFD code Fluent (version 15.0.7) is used to perform RANS simulations of flow over an idealized urban morphology in isothermal conditions, with the aligned array consisting of 7 × 6 buildings with a height of h (=0.15 m), and between building spacing equal to h in both the streamwise and spanwise direction. Hence, the numerical setup is selected to reproduce the conditions of the wind tunnel experiment of Brown et al. (2001). The Reynolds number of the flow is 3×10^4 based on the free stream velocity and building height. The same experimental data was recently used for validation of a large-eddy simulation code (Cheng and Porté-Agel 2015). The computational domain, shown in Fig. 1, has dimensions equal to $L_x \times L_y \times L_z$ 4.8 m × 1.8 m × 2.1 m. The structured grids with grid resolution of $N_x \times N_y \times N_z = 320 \times 120 \times 210$ grid points are tested, which correspond to a number of grid points covering the building of $(n_x \times n_y \times n_z) = 10 \times 10 \times 15$, respectively.

A turbulent inflow condition with a non-uniform (logarithmic) mean velocity profile is used at the inlet, as in the reference experiment. The inlet profile of the normalized mean streamwise velocity is compared with wind tunnel experiment and LES results, and is shown in Fig. 2. Symmetry boundary conditions are specified for

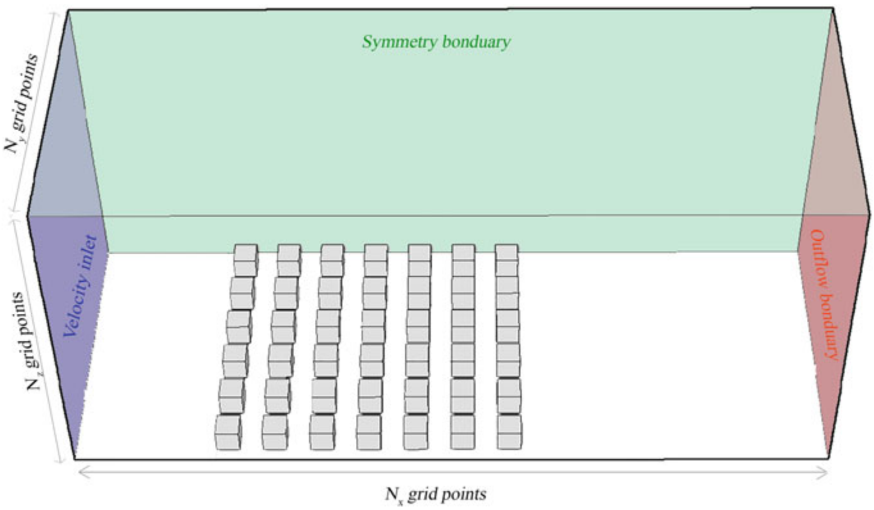

Fig. 1. The computational domain

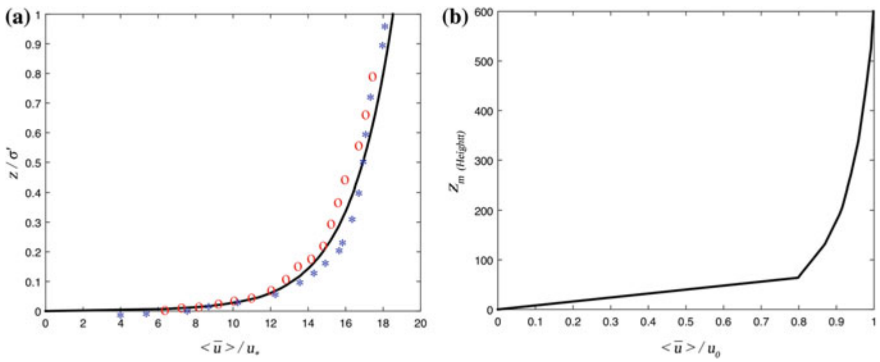

Fig. 2. Vertical inflow profiles of normalized mean streamwise velocity component **a** idealized urban canopy case and **b** semi-idealized high-rise buildings case. *Red circle symbols* wind tunnel experiment; *blue star symbols* LES; *black line* RANS

the top and sides of the computational domain (Franke et al. 2010). At the domain outlet, an outflow boundary condition is used. This implies that all streamwise derivatives of the flow variables are equal to zero at the outlet. A standard wall function based on the logarithmic law for smooth surfaces (Launder and Spalding 1974) is used at the upstream ground, downstream ground and at the surfaces of the buildings. The selected value of the sand-grain roughness height $k_s = 0.00014h$ (for the upstream ground) and $k_s = 0.014h$ (for the downstream ground and buildings surfaces) are calculated based on the relation $k_s = 9.793z_0/Cs$ (Blocken et al. 2012; Blocken 2015) where the roughness constant $C_s = 0.7$ (Tominaga 2015) and aerodynamic roughness length $z_0 = 10^{-3}h$ are used in order to reproduce the same conditions as in the wind tunnel experiment and LES. As suggested by the practical guidelines of CFD for flows in urban areas (Blocken et al. 2012; Blocken 2015; Franke et al. 2004, 2007; Tominaga et al. 2008), all transport equations are discretized using a second-order scheme. The COUPLED (Fluent 2013) algorithm is used to solve the momentum and pressure-based continuity equations.

Semi-Idealized High-Rise Building Case

As shown in Fig. 3, to perform RANS simulations of flow over semi-idealized high-rise buildings, the aligned 7 × 7 array, consisting of $l_x \times l_y$ equal to 50 m 50 m, rectangular prism buildings with differing heights of (=10 m), (=20 m), and (=50 m) for the very low-rise, low-rise and mid-rise buildings, respectively, are considered. Moreover, three simulations are performed for three different idealized high-rise morphologies with a height of (=200 m) which are implemented at the center of the semi-idealized urban canopy. The spacing between buildings is 20 m in both streamwise and spanwise directions. The computational domain has dimensions L_x $L_y \times L_z$ equal to 4800 m × 3400 m × 600 m. A turbulent inflow condition with a non-uniform (logarithmic) mean velocity profile is used at the inlet, as shown in Fig. 2.

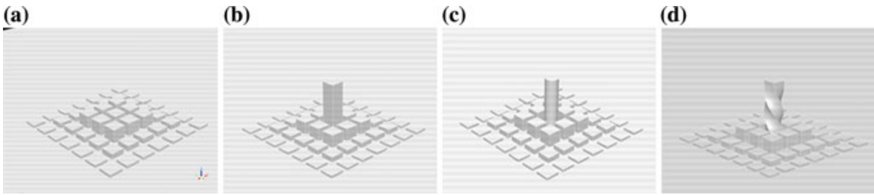

Fig. 3. Semi-idealized urban canopy **a** without a high-rise building (reference case), **b** rectangular prism high-rise morphology, **c** cylindrical high-rise morphology and **d** twisted high-rise morphology

Note that the remaining numerical setup of the simulations is similar to the one described in Section "Idealized Urban Canopy Case".

3 Results and Discussion

Vertical and Spanwise Profiles of the Idealized Urban Canopy

In this section, the normalized mean velocity simulated by the different RANS models are compared to the wind tunnel measurements of Brown et al. (2001) and the LES results of Cheng and Porté-Agel (2015) using a modulated gradient subgrid-scale (SGS) model (Lu and Porté-Agel 2010). The streamwise velocity components are denoted by (u). As shown in Fig. 4, all the RANS models reproduce the reverse flow at the top surface of the first idealized building fairly well for the mean velocity profiles. It is found that the RNG $k - \varepsilon$ model is not able to reproduce the reverse flow above and between buildings at the downstream positions from x_h = (1–4h), and a much smaller streamwise velocity is found in the aforementioned locations. In comparison, the two SST models show a slightly better prediction of the vertical profiles of streamwise velocities, which is related to the better performance of these models in adverse pressure gradient flow. In these grid conditions, the SST $\gamma - Re_\theta$ model shows the best overall prediction, followed by the SST $k - \omega$ model. The improved results of the SST $\gamma - Re_\theta$ is more obvious in spanwise velocity profiles at the downstream position of x_h = (6h). These results are consistent with the previous study of Kardan et al. (2016) that indicates that the SST models show better overall performance than the other RANS models tested for flows past an isolated building.

Vertical Profiles of Mean Velocity Around the Semi-idealized High-Rise Morphologies

In this section, three more simulations are conducted to analyze the impact of rectangular prism, cylindrical and twisting morphologies on the flow around and above the semi-idealized urban canopy, and the results are compared to a reference case where a high-rise building is absent. The SST $\gamma - Re_\theta$ turbulence model is selected based on

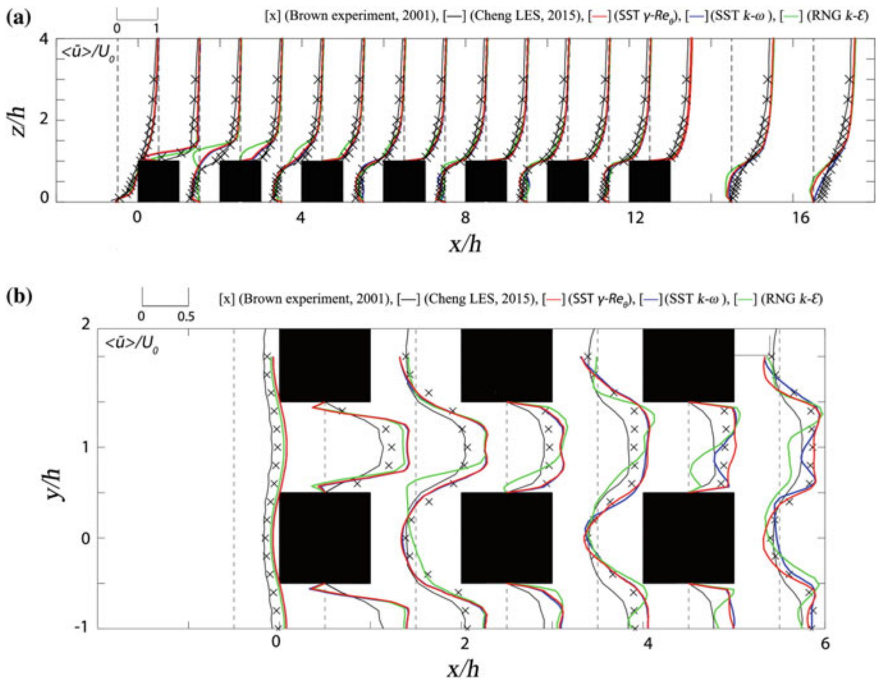

Fig. 4. **a** Vertical profiles at centerline of the idealized urban canopy and **b** spanwise profiles at $z = h/2$ of $\langle \bar{u} \rangle / U_0$. *Cross symbols* experiment; *black lines* LES; *red lines* SST $\gamma - Re_\theta$ model; *blue lines* SST $k - \omega$ model; *green lines* RNG $k - \varepsilon$ model

the results obtained in the previous section. The normalized mean velocity profiles at the center of the surrounding and high-rise buildings are projected from roof level to the domain height, and compared to that of the reference case as labeled and shown in Fig. 5.

It is found that there is symmetry between rows (a) and (c) of the results. For the upstream locations of (a, i) and (c, i), similar velocity patterns are found across the different high-rise morphologies, and that the convergence of these patterns is found at a height of (=300 m). It is worth mentioning that the velocity magnitudes upstream of the high-rise across the different morphologies are smaller than that of the reference case. It is also found that velocity magnitude is higher in the cylindrical high-rise morphology than the rectangular prism and twisted morphologies in these two locations. In the (b, i) building, all the high-rise morphologies introduce a velocity profile consisting of lower magnitudes when compared to the previously mentioned buildings. This is mainly due to the adverse pressure gradient flow that is induced by the presence of the high-rise building.

For the (a, ii) and (c, ii) buildings, similarity is found except for in the case of the twisted morphology, where some fluctuation is observed in the (a, ii) building. This is due to the irregular form of twisted geometries where opposite faces are not symmetrical. For the rectangular prism and cylindrical morphologies, the velocity

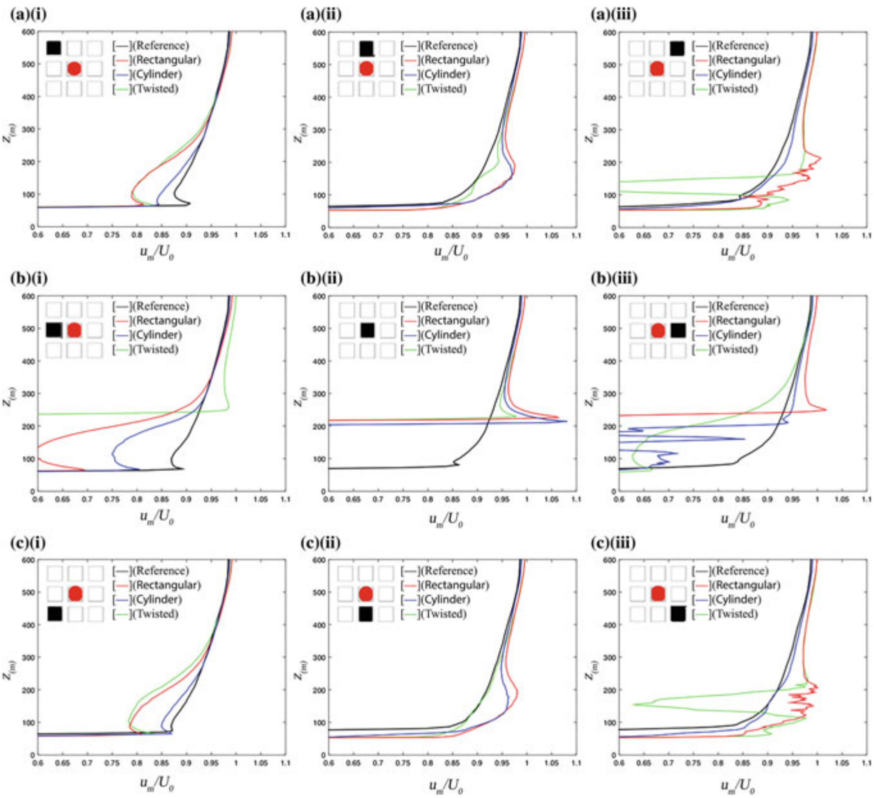

Fig. 5. Vertical profiles of the normalized mean velocity magnitude. *Black lines* reference case; *red lines* rectangular prism high-rise morphology; *blue lines* cylindrical high-rise morphology; *green lines* twisted high-rise morphology

magnitude profiles between (=50 m) and (=150 m) are significantly higher than in the reference case. The surrounding buildings downstream of the high-rise building are shown to be highly sensitive to the different types of high-rise morphologies. It is found that in (a, iii) and (c, iii) the twisted morphology velocity profile deviates the most from the reference case between (=50 m) and (=150 m), where the normalized velocity magnitude decreases to (=0.5) and (=0.62), respectively. The highest velocity magnitude across the simulations is found just above the high-rise building for the rectangular prism and cylindrical morphologies. This indicates that these two morphologies have higher potential to harvest wind energy from. However, this high velocity magnitude is not sustained, and about (=10 m) above the roof, decreases rapidly and begins to converge with the reference case.

Strong fluctuations in the vertical velocity profiles are found at (b, iii), directly downstream of the high-rise building. This indicates that the mentioned location is particularly sensitive to the morphology of the high-rise building. It is of interest to mention the differences in the vertical velocity profiles of the cylindrical and rectangular morphologies across the downstream region. In the cylindrical case, the buildings on either side of the high-rise exhibit a smooth profile similar to the reference case, whereas directly downstream of the high-rise, a large amount of fluctuation is observed. This is due to the fact that a cylindrical morphology encourages rapid re-combination of the separated flows. In the rectangular prism morphology, the velocity profile directly downstream of the high-rise building retains the shape of the profile at the high-rise itself, as it does not allow the separated stream flow to re-converge immediately. Instead, turbulent flow can be found downstream on either side of the high-rise building due to recirculation patterns found in the wake region of the building corner.

Comparison of Pressure Coefficient (C_P) and TKE Contours

Figure 6 shows the pressure coefficient distribution on the high-rise morphologies. From the results obtained, the maximum pressure coefficient is found in the case of the rectangular prism followed by the twisted and cylindrical morphologies. This indicates that the circular plan shape for tall buildings is more effective in reducing wind pressure than those of rectangular plan shapes.

In addition, the contours of the normalized turbulent kinetic energy (TKE) k/U_0^2 are also obtained along the centerline of the streamwise direction of the high-rise building morphologies, as can be seen in (Fig. 7).

In all cases, over-prediction of the TKE just above the high-rise buildings is found. Simulated patterns around the rectangular prism and twisted morphologies are more similar when compared with the cylindrical morphology, which relates to the shared rectangular plan shape of these buildings. It is worthwhile to mention that in the twisted high-rise morphology case, higher TKE is found around mid-rise buildings at upstream locations of the twisted tower, compared with those of rectangular prism and cylindrical morphologies. These results are consistent with those of the previous discussions in Section "Vertical Profiles of Mean Velocity Around the Semi-idealized High-Rise Morphologies" which indicates higher velocity fluctuation downstream of the twisted morphology.

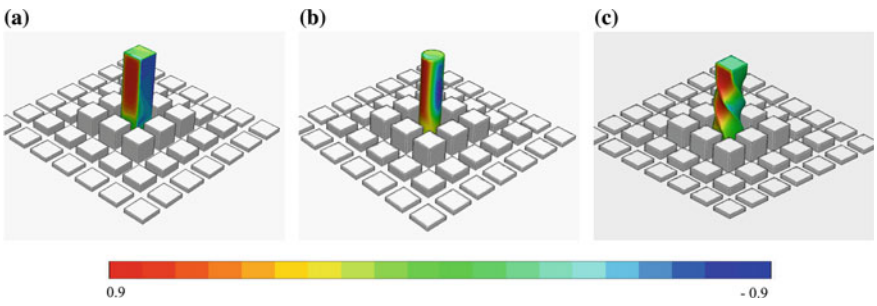

Fig. 6. Pressure coefficient distribution on **a** rectangular prism high-rise morphology, **b** cylindrical high-rise morphology and **c** twisted high-rise morphology

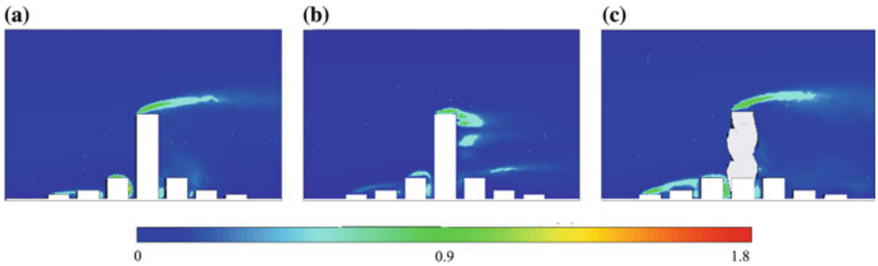

Fig. 7. Pressure coefficient distribution on **a** rectangular prism high-rise morphology, **b** cylindrical high-rise morphology and **c** twisted high-rise morphology

4 Summary

The present study assesses the performance of the RNG $k - \varepsilon$, SST $k - \omega$ and SST $\gamma - Re_\theta$ models for flow over an idealized urban canopy by comparing the simulation results with the wind tunnel measurements of Brown et al. (2001) and the large-eddy simulation results of Cheng and Porté-Agel (2015). The SST $k - \omega$ and SST $\gamma - Re_\theta$ models show improved predictions for the vertical and spanwise profiles of the mean velocity. It is found the computational costs of the SST models are significantly lower, and at least a hundred times faster, than LES. In addition, as the SST $\gamma - Re_\theta$ model is developed to simulate transitioning (from laminar to turbulent) flows, it can be particularly useful for flows around supertall buildings.

The SST $\gamma - Re_\theta$ model is used to conduct further simulations, which analyze the impact of high-rise morphologies on the flow around and above the semi-idealized urban canopy. The pressure coefficient distribution on high-rise buildings, normalized TKE contours and normalized mean velocity profiles simulated for the rectangular prism, cylindrical, and twisted morphologies are compared with the reference case, where a high-rise building is absent. It is found that different building morphologies can lead to very strong changes in velocity magnitude above the surrounding buildings. More specifically, the circular plan shape of tall building is more effective in reducing wind pressure compared with those of rectangular plan shapes. Amongst all surrounding buildings, those located directly upstream and downstream of the high-rise building were most affected by the differing morphology type. It is also found that the circular plan shape for tall buildings is more effective in reducing wind pressure compared to the rectangular plan shapes.

References

Blocken, B., Janssen, W.D., van Hooff, T.: CFD simulation for pedestrian wind comfort and wind safety in urban areas: general decision frame-work and case study for the Eindhoven University campus. Environ. Model. Softw. **30**, 15–34 (2012)

Blocken, B.: Computational fluid dynamics for urban physics: importance, scales, possibilities, limitations and ten tips and tricks towards accurate and reliable simulations. Build. Environ. **91**, 219–245 (2015)

Brown, M.J., Lawson, R.W., DeCroix, D.S., Lee, R.L.: Comparison of centerline velocity measurements obtained around 2D and 3D building arrays in a wind tunnel. Technical Report, Los Alamos National Laboratory, NM, pp. 7 (2001)

Cheng, W.C., Porté-Agel, F.: Adjustment of turbulent boundary-layer flow to idealized urban surfaces: a large-eddy simulation study. Bound. Layer Meteorol **50**, 249–270 (2015)

Fluent, A.: ANSYS fluent user's guide. Release 15.0 edn (2013)

Franke, J., Hellsten, A., Hirsch, C., Jensen, A.G., Krus, H., Schatzmann, M., Miles, P.S., Westbury, D.S., Wisse, J.A., Wright, N.G.: Recommendations on the use of CFD in wind engineering. In: van Beeck, J.E. (ed.) COST Action C14, Impact of Wind and Storm on City Life Built Environment. Von Karman Institute. Proceedings of the International Conference on Urban Wind Engineering and Building Aerodynamics, von Karman Institute, Sint-Genesius-Rode, Belgium (2004)

Franke, J., Hellsten, A., Schlu ̈nzen, H., Carissimo, B.: Best practice guideline for the CFD simulation of flows in the urban environment. COST action, pp. 51 (2007)

Franke, J., Hellsten, A., Schlu ̈nzen, H., Carissimo, B.: The best practise guideline for the CFD simulation of flows in the urban environment: an outcome of cost 732. In: Fifth International Symposium on Computational Wind Engineering, pp. 1–10 (2010)

Ferziger, J.H., Peric, M.: Computational methods for fluid dynamics, pp. 364. Springer, Berlin (1997)

Kardan, F., Cheng, W.C., Baverel, O., Porté-Agel, F.: An evaluation of recently developed RANS-based turbulence models for flow over a two-dimensional block subjected to different mesh structures and grid resolutions. E.G.U. 18 (2016)

Launder, B.E., Spalding, D.B.: The numerical computation of turbulent flows. Comput. Methods Appl. Mech. Eng. **3**, 269–289 (1974)

Langtry, R.D., Menter, F.R.: Correlation-based transition modeling for unstructured parallelized computational fluid dynamics. AIAA J. **47**, 2894–2906 (2009)

Liu, X., Niu, J., Kwok, K.C.S.: Evaluation of RANS turbulence models for simulating wind-induced mean pressures and dispersions around a complex-shaped high-rise building. Build. Simul. **6**, 151–164 (2013)

Liu, J., Niu, J.: CFD simulation of the wind environment around an isolated high-rise building: an evaluation of SRANS, LES and DES models. Build. Environ. **96**, 91–106 (2016)

Lu, H., Porté-Agel, F.: A modulated gradient model for large-eddy simulation: application to a neutral atmospheric boundary layer. Phys. Fluids **22**, 1–12 (2010)

Menter, F.R.: Two-equation eddy-viscosity turbulence models for engineering applications. AIAA J. **32**, 1598–1605 (1994)

Moonen, P., Defraeye, T., Dorer, V., Blocken, B., Carmeliet, J.: Urban physics: effect of micro-climate on comfort, health and energy demand. Front. Archit. Res. **1**(3), 197–228 (2012)

Nakayama, H., Takemi, T., Nagai, H.: LES analysis of the aerodynamic surface properties for turbulent flows over building arrays with various geometries. J. Appl. Meteorol. Climtol. **50**, 1692–1712 (2011)

Pope, S.B.: Turbulent flows, pp. 771. Cambridge University Press, Cambridge (2000)

Stankovic, S., Campbell, N., Harries, A.: Urban wind energy, pp. 200. Earthscan, Abingdon (2009)

Tominaga, Y., Mochida, A., Kataoka, H., Tsuyoshi, N., Masaru, Y., Taichi, S.: AIJ guidelines for practical applications of CFD to pedestrian wind environment around buildings. J. Wind Eng. Ind. Aerodyn. **96**, 1749–1761 (2008)

Tominaga, Y., Stathopoulos, T.: CFD simulation of near-field pollutant dispersion in the urban environment: a review of current modeling techniques. Atmos. Environ. **79**, 716–730 (2013)

Tominaga, Y.: Flow around a high-rise building using steady and un-steady RANS CFD: effect of large-scale fluctuations on the velocity statistics. J. Wind Eng. Ind. Aerodyn. **142**, 93–103 (2015)

Yakhot, Y., Orszag, S.A., Thangam, S., Gatski, T.B., Speziale, C.G.: Development of turbulence models for shear flows by a double expansion technique. Phys. Fluids A **4**, 1510–1520 (1992)